Dynamic Response Of Steel-Concrete Beams With Partial Interaction Due To Moving Loads

Respuesta Dinámica De Vigas De Acero-Hormigón Con Interacción Parcial Debido A Cargas En Movimiento

Authors

Mohamad Ali,[a,1], Mohamad El Dandachy[a,2], Ahmed M. Ellakany[a,b,3]

a) Faculty of Engineering, Beirut Arab University, Lebanon,
b) Faculty of Engineering, Alexandria University
(1): mohamad.ali@bau.edu.lb, (2): m.dandachy@bau.edu.lb, (3): ellakany@bau.edu.lb

ABSTRACT

Purpose *–The main purpose of this paper is to propose a numerical model, which represents the dynamic responses of elastic steel-concrete beams.*

Design/methodology/approach *–The numerical model is based on the lumped system with the combination of the transfer matrix method (TMM) and the analog beam method (ABM). The composite beams that are widely used in the construction of highway bridges are composed of an upper concrete slab and a lower steel beam, connected at the interface by shear transmitting studs. The field and point transfer matrices for the beam element of the elastic composite beams are derived. The present model is verified and applied to study the dynamic response of elastic composite beams subject to both moving force and mass. The effects of shear stiffness between the upper slab and lower beam and moving load velocity on the steel-concrete beams deflection are shown.*
Findings *–Results indicate that the maximum deflection in the composite beam subjected to moving load, is significantly affected by the level of interaction between sub-beams and by the load type and velocity.*

Originality/value *– Recently, a numerical model based on the lumped system with the combination of the TMM and the ABM was proposed to study the response of elastic steel-concrete beams with partial interaction, limited to static loading solely. In this study, the current proposed model is developed to study the dynamic response of steel-concrete beams with partial interaction due to moving loads of various velocities. The advantage of the proposed model, unlike previous models that are based on the combination of (TMM) and (ABM), is the ability to study the dynamic behavior of the elastic steel-concrete beams with various end and intermediate conditions and different types and velocities of moving loads.*

Key Words: *Numerical model, Lumped system, Steel-concrete elastic composite beams, Dynamic analysis.*

RESUMEN

Propósito –El objetivo principal de este artículo es proponer un modelo numérico que represente las respuestas dinámicas de vigas elásticas de acero-hormigón.

Diseño/metodología/enfoque –El modelo numérico se basa en el sistema concentrado con la combinación del método de matriz de transferencia (TMM, siglas en inglés) y el método de viga análoga (ABM, siglas en inglés). Las vigas compuestas que se utilizan ampliamente en la construcción de puentes de carreteras, están compuestas por una losa superior de hormigón y una viga inferior de acero, conectadas en la interfaz mediante montantes transmisores de cortante. Se derivan las matrices de transferencia de campo y de puntos para el elemento de viga de las vigas elásticas compuestas. El presente modelo se verifica y aplica para estudiar la respuesta dinámica de vigas compuestas elásticas sujetas tanto a fuerza como a masa en movimiento. Se muestran los efectos de la rigidez al corte entre la losa superior y la viga inferior y la velocidad de la carga en movimiento sobre la deflexión de las vigas de acero-hormigón.
Hallazgos: los resultados indican que la deflexión máxima en la viga compuesta sometida a carga en movimiento se ve significativamente afectada por el nivel de interacción entre las subvigas y por el tipo de carga y la velocidad.

Originalidad/valor – Recientemente, se propuso un modelo numérico basado en el sistema agrupado con la combinación del TMM y el ABM para estudiar la respuesta de vigas elásticas de acero-hormigón con interacción parcial, limitada únicamente a carga estática. En este estudio, se desarrolla el modelo propuesto actual para estudiar la respuesta dinámica de vigas de acero-hormigón con interacción parcial debido a cargas en movimiento de diversas velocidades. La ventaja del modelo propuesto, a diferencia de modelos anteriores que se basan en la combinación de (TMM) y (ABM), es la capacidad de estudiar el comportamiento dinámico de las vigas elásticas de acero-hormigón con diversas condiciones finales e intermedias y diferentes tipos y velocidades de cargas en movimiento.

Palabras clave*:* Modelo numérico, Sistema concentrado, Vigas compuestas elásticas de acero-hormigón, Análisis dinámico.

Editorial Note: Received: September 2023 Accepted: November 2023

1. INTRODUCTION

Steel-concrete composite beams, consisting of a concrete slab lying on top of a steel beam, are widely employed in structural applications. Shear connectors attach the two components to transmit the horizontal shear force between them. Slippage may possibly occur at the interface between the two parts of the composite beam in case of partial or no interaction. Integrating concrete and steel in one structure yield a favorable result in the world of construction combining the high tensile strength and ductility for steel, and the high compressive strength of concrete. The growing use of these beams in structural applications demands fundamental understanding of their mechanical behavior under moving loads as the dynamic responses cannot be ignored, especially in applications such as highway bridges in which the safety and carrying capacity are critical. Due to the dynamic nature of the loads to which these bridges are subjected to, become imperative to perform a proper analysis and gain a comprehensive understanding of the dynamic response of steel-concrete beams under moving loads.

Three approaches are considered to evaluate the dynamic response of elastic beams and steel-concrete composite beams: analytical, numerical, and experimental approaches. The complexity of the phenomenon limits the analytical studies to very simple cases until the 1950s when a one-dimensional numerical model to study the dynamic effect of moving loads on bridge behavior was presented [1]. Moreover, [2] explored the dynamic response of a simply supported beam by solving analytically the governing differential equation. The findings of the analytical solutions performed by [3] and [4] indicated that the dynamic deflection of the beam is 50% greater than its static deflection. Moreover, several methods of finite element analysis were proposed to analyze dynamic beam behavior such as Wilson's method and Newmark's method [5, 6]. The results of these studies agreed with those found analytically.

The dynamic response of steel concrete composite beams has been an area of great interest for researchers and engineers. Based on finite element modeling, a vibration analysis was performed on laminated composite beams experiencing moving loads based on a multilayered shear deformable beam element [7]. The dynamic model for two-layer partial interaction composite beams was solved with finite element simulations, applying Kant's higher-order beam kinematics [8]. The consideration of the slip between the members of the steel-concrete composite beam was taken by using Lagrange's formulation based on finite element modeling in [9]. A 3D finite element numerical model was developed to explore the bending behavior of high-strength steel–concrete composite beams that are simply supported [10]. Non-linear behavior is considered on both a geometric and a material level. Furthermore, [11], introduced a 3D finite element model and parametric study of the dynamic response of simply supported, horizontally curved composite steel I-girder bridges using the ANSYS program.

Some authors have established experimentally validated numerical models. For instance, [12] presented for beam type bridges, a flexibility matrix identification approach based on induced responses by moving vehicle. The analytical mode decomposition is applied to extract the quasi-static component response of the induced responses by moving vehicle, and the influence line of the measurement point is derived by polynomial fitting. Comparative analysis between the numerical model and experimental data is conducted. Moreover, [13] performed a numerical analysis on the shear behavior of perforated transverse angle shear connectors (PTACs) based on finite element modelling. The FE model was based on the experimental results [14].

Many researchers have conducted experiments to gain scientific knowledge vis-à-vis the behavior of steel-concrete composite beams. On the one hand, [15] have experimentally investigated the influence of shear connectors on the behavior of the steel-concrete composite beams under cyclic loading. An experimental campaign to assess the shear behavior of transverse angle shear connectors in steel-concrete composite girders was conducted by [14]. [16] for instance, investigated in their experiments on dynamic behavior of steel – concrete beams under harmonic force, the influence of shear connection degree, the static load components, load amplitude and frequency, on the slip and deflection at various measuring points.

Several methods could be considered to analyze the behavior of steel-concrete beams in partial interaction. For instance, the static behavior of composite beams with partial interaction was analyzed using a generic model developed by [17] based on the technique of Newmark, Siess and Viest. The Analog Beam Method (ABM) can be used to analyze the behavior of the real composite beam. The deformation, bending moment and shear force that represent the behavior of the real composite beam, can be analyzed using the ABM by concentrating the shear deformation in a thin layer, namely the shear layer, to ensure that the correct stiffness is used in this layer [18, 19]. This method was utilized in many studies [20, 21, 22]. In addition, the Transfer Matrix Method (TMM), initially developed [23], could be applied in various engineering applications. The TMM is relatively less demanding, and its implementation is simple compared to other numerical models. On top of that, it could account for intermediate conditions, e.g., flexible, rigid supports and internal hinges.

The combination of the TMM and ABM was created to improve the modeling of static and dynamic responses in structures, specifically in steel-concrete composites [18, 19, 20, 23]. The transfer matrix method (TMM) combined with the analog beam method (TMABM) was employed to numerically predict the natural frequencies for elastic composite beams with different intermediate conditions. Based on this work, an exact dynamic field transfer matrix for evaluating the natural frequencies of composite beams has been suggested [20]. Further elaboration on the dynamic response of composite beams has included the application of the Riccati matrix method to evaluate higher natural frequencies of elastic composite beams with simple supports [24]. Moreover, the end shear restraint has also been included in the ABM [25]. In all aforementioned studies, models consider the distributed beam mass system. However, a numerical model based on the lumped system with the combination of the TMM and the ABM was proposed recently to study the static response of elastic steel-concrete beams with partial interaction [26]. The lumped system, unlike the case of distributed mass system, allows for studying the dynamic behavior of the elastic steel-concrete beams with various end and intermediate conditions and for different types of moving loads.

The objective of this study is to propose a numerical model based on a lumped system to calculate the dynamic behavior of one span elastic composite beam under moving load, by combining the ABM with the TMM. The developed model is applicable for studying dynamic responses of steel-concrete elastic composite beams with different end conditions, considering the effect of partial shear interactions. The model is checked by comparing the results with those obtained by [27, 28]. Afterward, the proposed model is applied to obtain the normalized deflection of the composite beam at different velocities of the moving load with different levels of interaction between the concrete slab and steel beam. In further contributions, the lumped mass model will be developed and used to investigate the dynamic behavior of the elastic composite beams subjected to moving vehicles with end shear restraint and intermediate support.

2. NUMERICAL MODELS

2.1. The Governing Equations of the Elastic Composite Beam Element

The beam model used in this investigation is a composite steel-concrete beam, which is composed of an upper concrete slab and a lower steel beam. This type of beam is commonly used in highway bridges. The typical type of elastic steel-concrete beam and its coordinate system are shown in Figure 1. The composite beam is subjected to a load (ML), moving at a velocity of v.

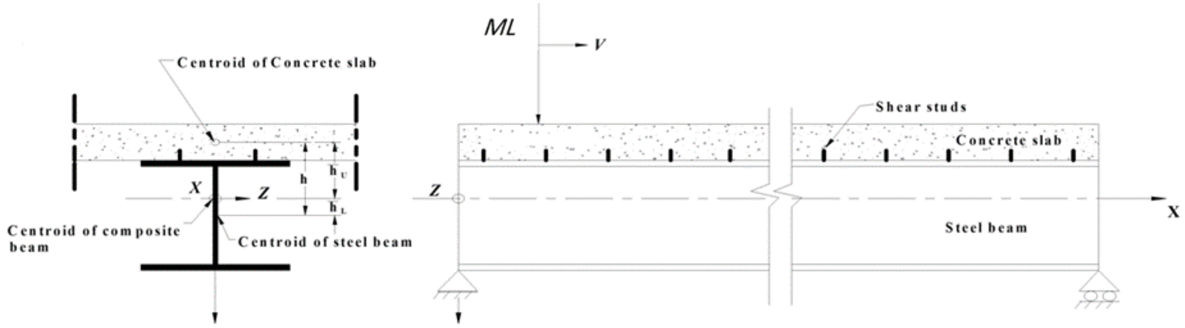

***Figure 1**: Coordinate system of a typical steel-concrete beam.*

The general theory of the analog beam method was proposed in [18] then later developed in [19]. The analog beam is thought of as composed of two sub-beams, called the upper and the lower beams. The method of analysis is based on two kinematic assumptions:

1. Each sub-beam behaves separately as a simple beam, i.e., the shear deformation within the sub-beams is neglected, so the shear deformation is concentrated in a thin layer called shear layer.
2. The vertical displacement of the concrete slab and the steel beam is the same.

For more details, the basic equations for an elastic composite beam are presented in [24]. It should be pointed out that the axial forces in the sub-beams are neglected. The state of forces and displacements of beam element is illustrated in Figure 2. For the elastic composite beam element shown in Figure 1, the equation of total bending moment is:

$$M = M_t + M_c \tag{1}$$

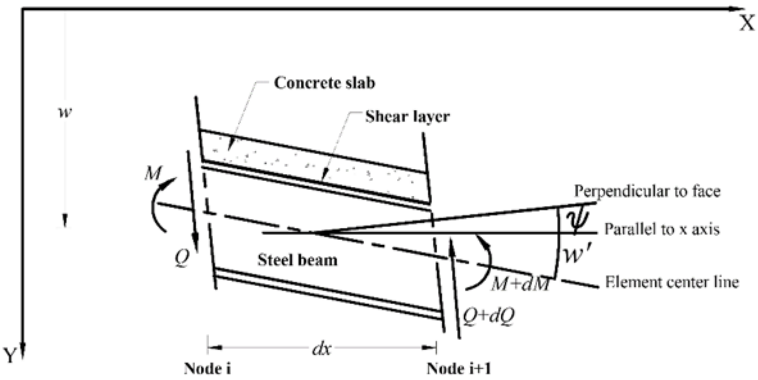

***Figure 2**: Forces and displacements of beam element.*

Where M_t is identified as the bending moment in the beam from what is called its "truss action", i.e., from the axial force in the sub-beams and M_c represents the combined bending moment from the individual beam action of the sub-beams.

$$M_t = (EI)_t \frac{d\psi}{dx} \quad (2\text{-a})$$

$$M_c = -(EI)_c \frac{d^2w}{dx^2} \quad (2\text{-b})$$

ψ, represent the slope due to slippage between the two sub-beams, w is the vertical deflection of the composite beam and, $(EI)_t$ and $(EI)_c$ are the bending stiffness of the beam components as if no interaction occurs, and of the truss component accounting for interaction, respectively. Equation (1) can be rewritten as:

$$M = (EI)_t \frac{d\psi}{dx} - (EI)_c \frac{d^2w}{dx^2} \quad (3)$$

The horizontal shear force (q) in the shear layer, which acts at the interface between the upper concrete slab and lower steel beam, can be expressed, according to [18], as:

$$q = kh^2 \left(\psi + \frac{dw}{dx}\right) \quad (4)$$

Where k is the shear stiffness of the shear layer and h is the distance between the centroids of the sub-beams (the perpendicular distance between the local z-axes). Similarly, the total shear force Q can also be thought of as having two components such as

$$Q = Q_t + Q_c \quad (5)$$

Where:

$$Q_t = kh^2\left(\psi + \frac{dw}{dx}\right) \text{ and } \quad Q_c = (EI)_c \frac{d^3w}{dx^3} \quad (6)$$

Then, the expression for ψ can be written as:

$$\psi = \frac{1}{kh^2}Q - \frac{1}{kh^2}\frac{dM_c}{dx} - \frac{dw}{dx} \quad (7)$$

Differentiation of equation (7) and substitution in equation (1) yield:

$$M = \frac{(EI)_t}{kh^2}\frac{dQ}{dx} + \frac{(EI)_t(EI)_c}{kh^2}\frac{d^4w}{dx^4} - (EI)\frac{d^2w}{dx^2} \quad (8)$$

Where, $(EI) = (EI)_t + (EI)_c$

2.2. Field Transfer Matrix

In case of a lumped system, the load of the beam element is concentrated at the two end points, called nodes, or point elements, and the beam element between the two nodes is called field element. Figure 3 illustrates a lumped mass beam element with the state of loads. The equilibrium considerations, for the field element, give the equations:

$$\frac{dQ}{dx} = 0 \qquad \text{and} \qquad Q = \frac{dM}{dx} \tag{9}$$

Taking the second derivative of equation (8) with respect to x and bounding with equation (9), the governing equation is expressed as:

$$\frac{d^6w}{dx^6} - \mu^2 \frac{d^4w}{dx^4} = 0 \tag{10-a}$$

Where:

$$\mu^2 = \frac{kh^2(EI)}{(EI)_c(EI)_t} \tag{10-b}$$

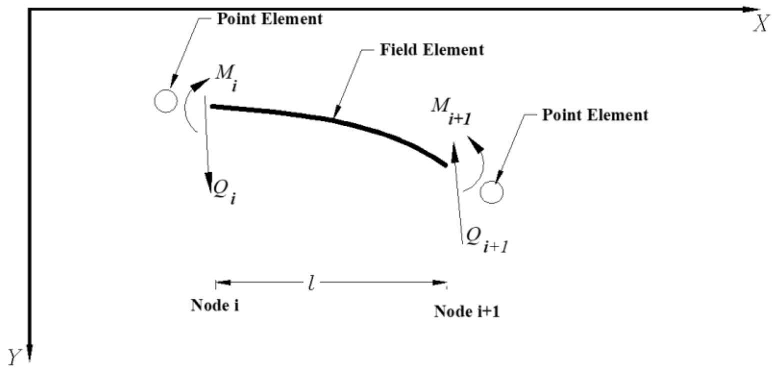

***Figure 3**: Lumped mass element.*

The solution of equation (10-a) is:

$$w(x) = C_1 + C_2x + C_3x^2 + C_4x^3 + C_5 \cosh \mu x + C_6 \sinh \mu x \tag{11}$$

From C_1 to C_6 are six constants. Substituting from equation (11) into the equations of w', ψ, M_t, M_C *and* Q then rewriting the obtained equations in the extended matrix form as:

$$\begin{bmatrix} w \\ w' \\ \psi \\ M_t \\ M_c \\ Q \\ 1 \end{bmatrix} = \begin{bmatrix} 1 & x & x^2 & x^3 & \cosh\mu x & \sinh\mu x & 0 \\ 0 & 1 & 2x & 3x^2 & \mu \sinh\mu x & \mu\cosh\mu x & 0 \\ 0 & -1 & -2x & -\frac{6(EI)_t}{kh^2} - 3x^2 & \beta_1 \sinh\mu x & \beta_1\cosh\mu x & 0 \\ 0 & 0 & -2(EI)_t & -6(EI)_t x & \beta_2\cosh\mu x & \beta_2 \sinh\mu x & 0 \\ 0 & 0 & -2(EI)_c & -6(EI)_c x & \beta_3\cosh\mu x & \beta_3\sinh\mu x & 0 \\ 0 & 0 & 0 & -6(EI) & \beta_4\sinh\mu x & \beta_4\cosh\mu x & 0 \\ 0 & 0 & 0 & 0 & 0 & 0 & 1 \end{bmatrix} \begin{bmatrix} C_1 \\ C_2 \\ C_3 \\ C_4 \\ C_5 \\ C_6 \\ 1 \end{bmatrix} \tag{12}$$

or

$$\{SV(x)\} = [D(x)]\{C\}$$

Where:

$$\beta_1 = \frac{\beta_4}{kh^2} + \frac{(EI)_c}{kh^2} - \mu,\ \ \beta_2 = (EI)_t\mu\beta_1,\ \ \beta_3 = -(EI)_c\mu^2 \ \text{ and } \ \beta_4 = \frac{(EI)_t(EI)_c}{kh^2}\mu^5 - (EI)\mu^2$$

For the beam element between two nodes *i* and *i+1* (see Figure 2 and Figure 3), the state vectors at both sides are $\{SV\}_i^R$ and $\{SV\}_{i+1}^L$ for x=0 and x= ℓ respectively, where ℓ is the length of the beam element. Then it can be written the following:

$$\{SV\}_i^R = \{SV(0)\} = [D(0)]\{C\} \quad \text{and} \quad \{SV\}_{i+1}^L = \{SV(\ell)\} = [D(\ell)]\{C\} \tag{13}$$

Eliminating the vector of constants $[C]$ from equations (13), yields:

$$\{SV\}_{i+1}^L = [MEFTM]\{SV\}_i^R \tag{14}$$

Where $[MEFTM]$ is called the Massless Extended Field Transfer Matrix for the elastic composite beam element.

2.3. Point Transfer Matrices

2.3.1. Point Transfer Matrix For Static Response

In the case of static response, the load is concentrated at the two ends called point elements. Displacements, slopes and moments are equal at both sides of the point element. The equilibrium consideration for shear force gives the equation:

$$dQ_{i+1} = -(W\ell/2) \tag{15}$$

Where, W is the weight of the beam per unit length, then the Static Extended Point Transfer Matrix $[SEPTM]$ relates between the state vectors $\{SV\}_{i+1}^R$ and $\{SV\}_{i+1}^L$ at both sides of point element i+1 is:

$$[SEPTM] = \begin{bmatrix} 1 & 0 & 0 & 0 & 0 & 0 & 0 \\ 0 & 1 & 0 & 0 & 0 & 0 & 0 \\ 0 & 0 & 1 & 0 & 0 & 0 & 0 \\ 0 & 0 & 0 & 1 & 0 & 0 & 0 \\ 0 & 0 & 0 & 0 & 1 & 0 & 0 \\ 0 & 0 & 0 & 0 & 0 & 1 & -\frac{w\ell}{2} - F_m \\ 0 & 0 & 0 & 0 & 0 & 0 & 1 \end{bmatrix} \tag{16-a}$$

Where:

$$\{SV\}_{i+1}^R = [SEPTM]\{SV\}_{i+1}^L \tag{16-b}$$

and

$$F_m = P\,\delta(x_{i+1} - \xi_{i+1}) \tag{16-c}$$

P represents the value of moving force and δ is the Dirac function, x_{i+1} and ξ_{i+1} are the coordinates from the left support to station $i+1$ and to the moving force respectively.

2.3.2. Point Transfer Matrix For Free Vibration

The distributed mass m of the beam is concentrated at the point element and according to the equilibrium consideration of the shear force is:

$$dQ_{i+1} = \left(\frac{m\ell}{2}\right)\ddot{w}_{i+1} \tag{17}$$

Where, $\ddot{w}_{i+1} = -{\omega_n}^2 w_{i+1}$ is the acceleration of the lumped mass at point i+1, and $w = sin\, \omega_n\, t$. From (17), the Free Vibration Extended Point Transfer Matrix [FVEPTM], that is used to compute the fundamental frequencies ω_n and the corresponding period, is:

$$[FVEPTM] = \begin{bmatrix} 1 & 0 & 0 & 0 & 0 & 0 & 0 \\ 0 & 1 & 0 & 0 & 0 & 0 & 0 \\ 0 & 0 & 1 & 0 & 0 & 0 & 0 \\ 0 & 0 & 0 & 1 & 0 & 0 & 0 \\ 0 & 0 & 0 & 0 & 1 & 0 & 0 \\ \dfrac{-m\ell {\omega_n}^2}{2} & 0 & 0 & 0 & 0 & 1 & 0 \\ 0 & 0 & 0 & 0 & 0 & 0 & 1 \end{bmatrix} \tag{18}$$

The determination of the fundamental frequency ω_1 is essential for the setting of a convenient time interval Δt of the load to move from a node to the next one [20, 24].

2.3.3. Point Transfer Matrix For Dynamic Response Due To Moving Load

The point matrix connecting $\{SV\}_{i+1}^{R}$ with $\{SV\}_{i+1}^{L}$ is found by noting that the deflection, slope, and moment are continuous across the concentrated mass m_{i+1}. The inertial force IF_{i+1}, and the external moving load ML cause a discontinuity in the shear. Therefore, it could be written as follows:

$$Q_{i+1}^{R} = Q_{i+1}^{L} + IF_{i+1} - ML\; \delta(x_{i+1} - \xi_{i+1}) \tag{19}$$

The equation of the inertia force of point mass at the node i+1 is:

$$IF_{i+1} = m_i \ell_i \ddot{w}_{i+1} \tag{20}$$

The equilibrium equation at node i+1 at time $t + \Delta t$, where Δt is the time interval of the load to move from a node to next one, is:

$$Q_{i+1}^{R}(t+\Delta t) = Q_{i+1}^{L}(t+\Delta t) + IF_{i+1}(t+\Delta t) - ML\; \delta(x_{i+1} - \xi_{i+1}) \tag{21}$$

There are several convenient methods to express the velocity $\dot{w}_{i+1}$ and the acceleration $\ddot{w}_{i+1}$ at time $t + \Delta t$ in terms of time t. One of the unconditionally stable direct integration methods is the Newmark β method. Based on $\beta = \frac{1}{4}$ and $< \frac{T}{20}$, where $T = \frac{2\pi}{\omega_1}$, the equation of forward integration of the velocity and acceleration are:

$$\dot{w}(t+\Delta t) = \frac{2}{\Delta t}[w(t+\Delta t) - w(t)] - \dot{w}(t) \tag{22-a}$$

$$\ddot{w}(t+\Delta t) = \frac{4}{\Delta t^2}[w(t+\Delta t) - w(t)] - \frac{4}{\Delta t}\dot{w}(t) - \ddot{w}(t) \tag{22-b}$$

From equations (21) and (22-b), the point matrix, which relates the state vectors at both sides of point element considering the moving load effect, takes the form:

$$[DEPTM]=\begin{bmatrix} 1 & 0 & 0 & 0 & 0 & 0 & 0 \\ 0 & 1 & 0 & 0 & 0 & 0 & 0 \\ 0 & 0 & 1 & 0 & 0 & 0 & 0 \\ 0 & 0 & 0 & 1 & 0 & 0 & 0 \\ 0 & 0 & 0 & 0 & 1 & 0 & 0 \\ DEPTM(6,1) & 0 & 0 & 0 & 0 & 1 & DEPTM(6,7) \\ 0 & 0 & 0 & 0 & 0 & 0 & 1 \end{bmatrix} \quad (23)$$

For the case of moving force $(ML = P)$, the elements of the matrix [DEPTM] could be written as follows:

$$DEPTM(6,1) = \frac{4}{\Delta t^2}(m\ell) \quad (24)$$

$$DEPTM(6,7) = -m\ell\left\{\frac{4}{\Delta t^2}w(t) + \frac{4}{\Delta t}\dot{w}(t) + \ddot{w}(t)\right\} - P\,\delta(x_{i+1} - \xi_{i+1}) \quad (25)$$

On the other hand, for the case of moving mass $(ML = Mg)$, the elements of the matrix [DEPTM] could be written in this case as follows:

$$DEPTM(6,1) = \frac{4}{\Delta t^2}\{m\ell + M\,\delta(x_{i+1} - \xi_{i+1})\} \quad (26)$$

$$DEPTM(6,7) = -\left(m\ell + M\,\delta(x_{i+1} - \xi_{i+1})\right)\left\{\frac{4}{\Delta t^2}w(t) + \frac{4}{\Delta t}\dot{w}(t) + \ddot{w}(t)\right\} - Mg\,\delta(x_{i+1} - \xi_{i+1}) \quad (27)$$

Where M is the mass of the load and g is the gravitational acceleration.

2.4. Transfer Matrix Scheme

The actual beam is divided into N massless field elements and N+1 point concentrated masses. The properties of the composite beam elements, such as load density, moment of inertia, shear stiffness and modulus of elasticity are assumed as constants. Applying the transfer matrix method for the beam system, the relation between the state vectors at the left support SL and the right support SR is:

$$\{SV\}_{SR} = [TM]\{SV\}_{SL} \quad (28\text{-a})$$

Where, $[TM]$ is the overall transfer matrix, which can be easily calculated by sequential multiplication of the field transfer matrix and the point transfer matrix from element 1 to element N according to the type of loading: static/dynamic or force/mass.

2.5. Boundary Conditions At The Ends Of The Beam

After the calculation of the overall transfer matrix [TM] is completed, the boundary conditions at both end supports of the beam are applied to calculate the unknown state vector elements at both ends. The boundary conditions for various types of beam end support are summarized in Table I, as indicated by [18].

***Table 1**: Boundary conditions at end supports.*

Type of end support	Corresponding boundary conditions
Hinged	w = 0.0, M_t =0.0 and M_c = 0.0
Fixed	w = 0.0, ψ = 0.0 and M_c = 0.0
Free	M_t = 0.0, M_c = 0.0 and Q = 0.0

The matrix multiplication scheme is applied to find the displacements and forces at node n of the beam system as following:

$$\{SV\}_n = [PM]_n \dots\dots\dots [FM]_2\,[PM]_2\,[FM]_1\,\{SV\}_{SL} \qquad (28\text{-b})$$

Where: $[PM]$ is the point matrix and $[FM]$ is the field matrix.

3. NUMERICAL VERIFICATION

To examine the accuracy of the present lumped model, the dynamic deflections of elastic composite beams subjected to moving load are calculated and compared with those obtained by [27] for the case of one span and [28] for the case of three spans.

3.1. Numerical Verification On One Span Beam

The numerical verification is hereby performed on a single span, simply supported beam of length (L) of 1 m, subjected to a moving load (P) of 1 kN at a velocity v of 0.2 m/s as shown in Figure 4. The density of the material is considered equal to 1 t/m. The rigidity of the beam (EI) is chosen equal to 1 $kN.m^2$. A complete interaction between sub-beams is set in the model to numerically represent this case study.
Mid-point displacements versus time (s), given by the current model, compared to the ones obtained by [27], are shown in Figure 5. The results indicate a good agreement between the two methods.

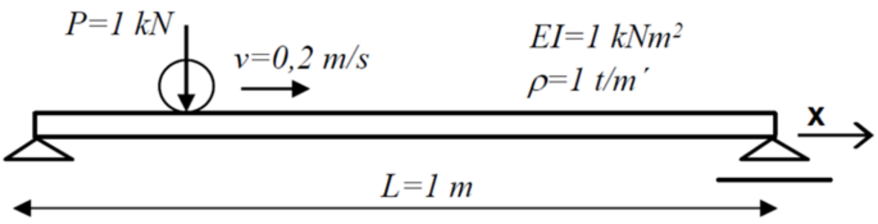

***Figure 4**: A schematic of the one span beam [27].*

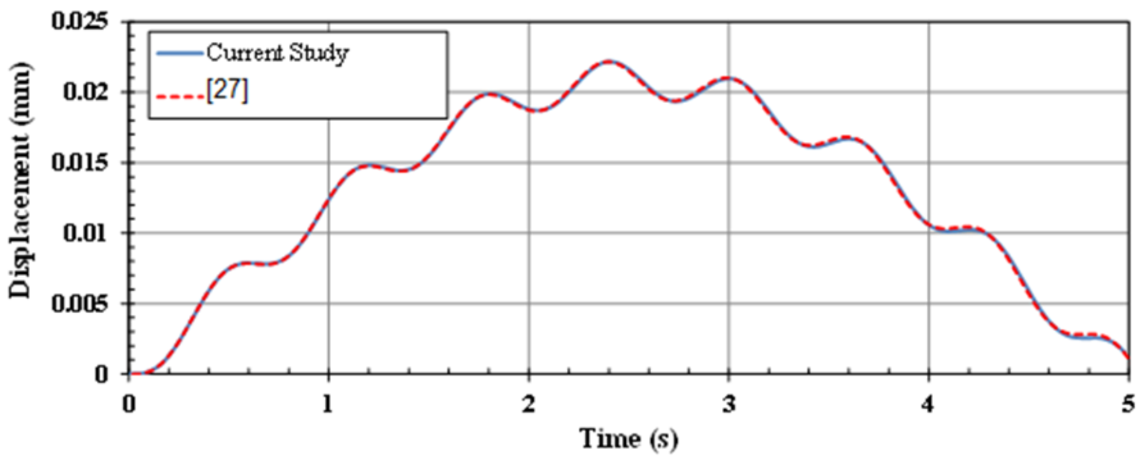

***Figure 5**: Mid-point displacement of one span beam due to moving load.*

3.2. Numerical Verification On A Three-Span Beam

The numerical verification of the current model is carried out on a three-span stepped beam subjected to a single load of P equal to 9.81 kN, moving at a speed of 34 m/s [28]. Figure 6 shows the drawing of the continuous three-span beam. The continuous beam has a linear density of 1000 kg/m and three spans of 20 m length each. The flexural rigidity is set equal to EI of 1.96 $GN.m^2$ for the two beams at sides and is set equal to $2EI$ of 3.92 $GN.m^2$ for the central beam. Intermediate supports at $x = 20\,m$ and at $x = 40\,m$ were dealt with in the current numerical model as discussed in [20].
Mid-point displacements versus time (s), given by the current model, compared to the ones obtained by [28], are shown in Figure 7. It shows that a good agreement is obtained.

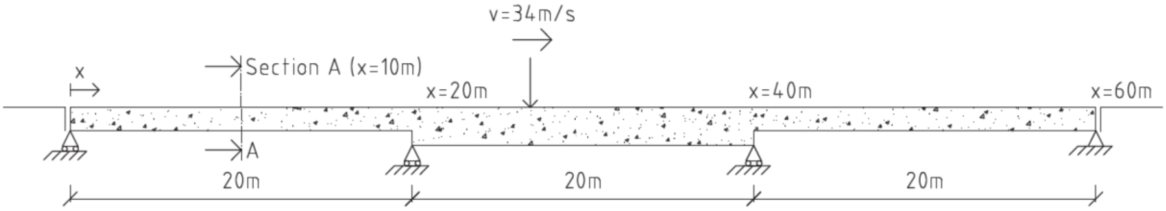

Figure 6: *Drawing of the three-span continuous beam under a single moving load [28].*

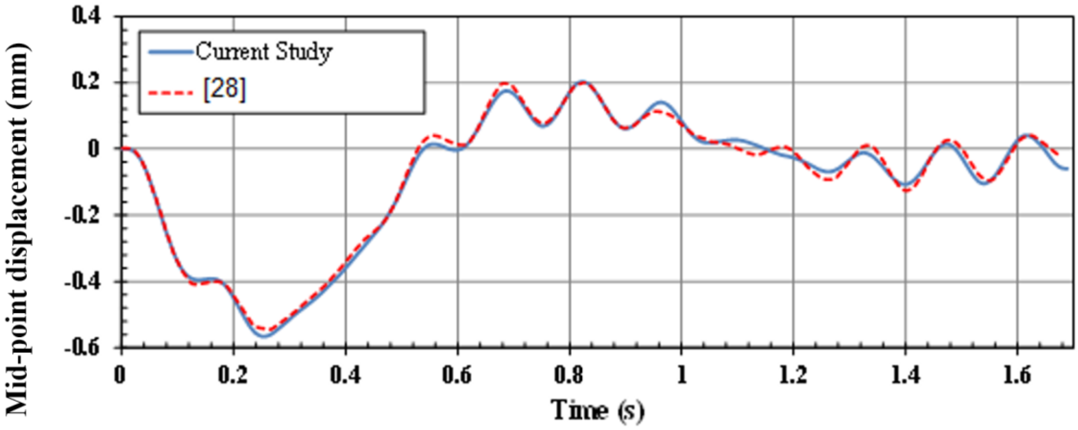

Figure 7: *Verification of the present numerical model using the results obtained in [28]*

4. PARAMETRIC STUDY

The parametric study is conducted on a simply supported elastic composite beam of length L, subjected to a moving load ML, (a force P or a mass M), moving at a velocity v (as shown in Figure 1). The aim is to investigate the influence of the composite beam parameters and the moving load velocity on the dynamic response of the steel concrete composite beam.
Static responses of the composite beam for different levels of interaction between the sub-beams are already addressed in [26]. The dynamic behavior of the steel concrete composite beam is significantly influenced by the load type, its velocity, flexural rigidity (EI) and the bending stiffness ratio η:

The parametric study is conducted on a simply supported elastic composite beam of length L, subjected to a moving load ML, (a force P or a mass M), moving at a velocity v (as shown in Figure 1). The aim is to investigate the influence of the composite beam parameters and the moving load velocity on the dynamic response of the steel concrete composite beam.
Static responses of the composite beam for different levels of interaction between the sub-beams are already addressed in [26]. The dynamic behavior of the steel concrete composite beam is significantly influenced by the load type, its velocity, flexural rigidity (EI) and the bending stiffness ratio η:

$$\eta = \frac{(EI)_t}{(EI)_c} \qquad (29)$$

The type of boundary conditions at both end of the beam, and the level of interaction between two sub-beams. This parametric study focuses on the effect of specific parameters, such as, the load type, its velocity and level of interaction on the dynamic behavior of the steel concrete composite beam. Therefore, it is convenient to introduce the following non-dimensional parameters:

$$\zeta = \frac{(EI)}{kh^2L^2} \qquad (30)$$

$$\delta = \frac{\omega}{\omega_{max}} \qquad (31)$$

$$\Delta = \frac{x}{L} \qquad (32)$$

Where w_{max} is the mid-point static deflection when no interaction between the sub-beams is considered, i.e., *k*=0. The dynamic deflection w is calculated at the mid-point for various locations of the load. Additionally, δ and Δ are the normalized deflection and distance, which indicates the location of the load on the beam, respectively. The dimensionless parameter ζ expresses the level of interaction between the two sub-beams of the composite beam. A wide range of values for ζ is possible, corresponds to complete interaction (i.e. no slip occurs between the two sub-beams) and, $\zeta = \infty$ corresponds to no interaction (as if there are no shear studs connecting the two sub-beams). The parameter ζ defined hereby, resembles to the parameter λ, introduced by [29], which represents the ratio of the actual number of stud connections in a shear span, to the least number of stud connectors in a shear span in a full-shear connection beam.

Therefore, $\zeta = 0$ is equivalent to $\lambda = 1$, and $\zeta = \infty$ corresponds to $\lambda = 0$. For a typical composite beam, the bending stiffness ratio η varies from about 0.2 to 1.4 [18]. The lower values of η correspond to cases of thick slab and small beam. Conversely, higher values correspond to cases where the concrete slab is thin, and the steel beam is large. In the following examples, the bending stiffness ratio η is considered equal to 1.

4.1. Dynamic Analysis Of Steel Concrete Composite Beam Subjected To Moving Load

The normalized deflections of a simply supported steel concrete composite beam, subjected to static load, moving force, or moving mass, for various velocities of the force/mass and for several level of interactions, are depicted in Figures 8 and 9. The calculations of the normalized deflections are based on the transfer matrix scheme (section 2-4) that is developed by using the terminologies of point transfer matrices and field transfer matrix (section 2.3 and 2.2 respectively).

Three load velocities of 60, 90 and 120 km/h and four levels of interaction of 0, 2, 20 and ∞ between sub-beams, are adopted in the dynamic analysis. Figures 8 show results of normalized deflections for the cases of static and moving force. The comparison between normalized deflection of moving force and moving mass is shown in Figures 9. The three velocities were selected to show how the normalized deflection undulates in the case of dynamic force around the results of static force that is observed in figure 8, where the wave lengths increase proportionally to the velocity. We can see that curves of the normalized deflection are clearly dependent on the value of the level of interaction (ζ) specifically between its smallest and largest value. For the intermediate values of ζ (2 and 20), ζ= 2 was chosen because its corresponding curve represents an average curve of normalized deflection between extreme cases (0 and ∞). Starting from the value of 20 for ζ the normalized deflection began to be less sensitive.

Expectedly, it is observed that in the case of complete interaction between the upper concrete slab and lower steel beam (ζ=0), the composite beam exhibits the lower deflection among all other cases, in both, static and dynamic analyses. Moreover, when the level of interaction between the sub-beams is reduced (ζ>0), the composite beam deflection increases, and its maximum value occurs when ζ=∞. Moreover, due to the dynamic nature of the load, it is observed that the normalized deflections, in case of moving load or moving mass (as shown in Figures 8 and 9), present a fluctuate behavior with respect to the case of static load. These fluctuations become more significant for lower levels of interaction between sub-beams and for higher moving load velocities. The highest increase in the maximum deflection due to dynamic nature of the moving force is found equal to approximately 18 % for the case of no interaction and for load velocity of 120 km/h as shown in Figure 8 (c). The maximum dynamic deflection conversely to the case of static loading, might not occur when the moving load is located at the mid-point of the beam because the dynamic response is influenced by the inertial effects of the masses involved, including the mass of the bridge and the moving mass. It occurs when the moving load has reached the vicinity of the mid-point, due to dynamic effects. Regarding the case of moving mass, it is shown that the highest increase in the maximum deflection due to dynamic nature of the moving mass is found equal to approximately 16 % for the case of no interaction and for load velocity of 90 km/h only (whereas it was 120 km/h for the case of moving load) as shown in Figure 9 (b). In addition, the value of maximum deflection is found when the moving mass is near, but not the same, compared to the case of moving force, as shown in Figure 9.

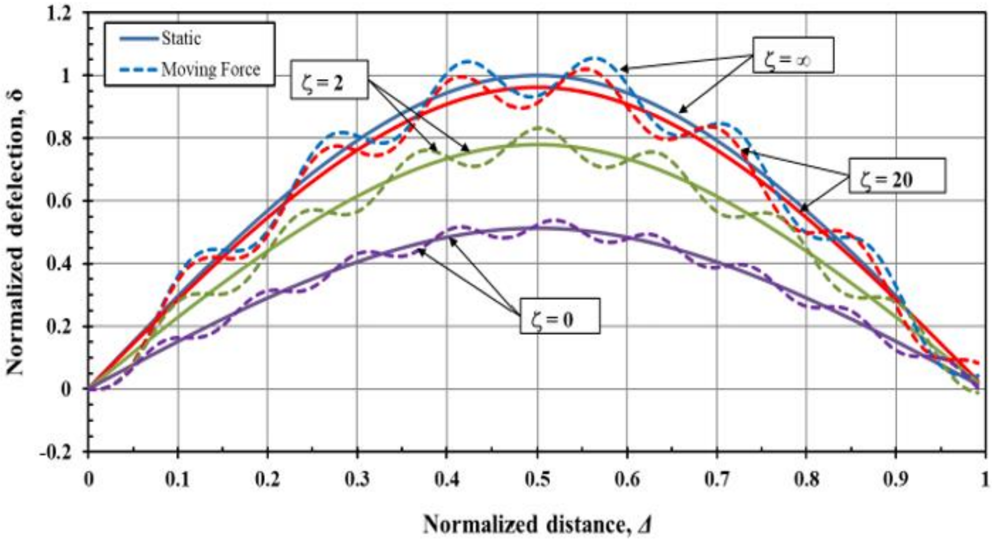

(a) Velocity = 60 km/h

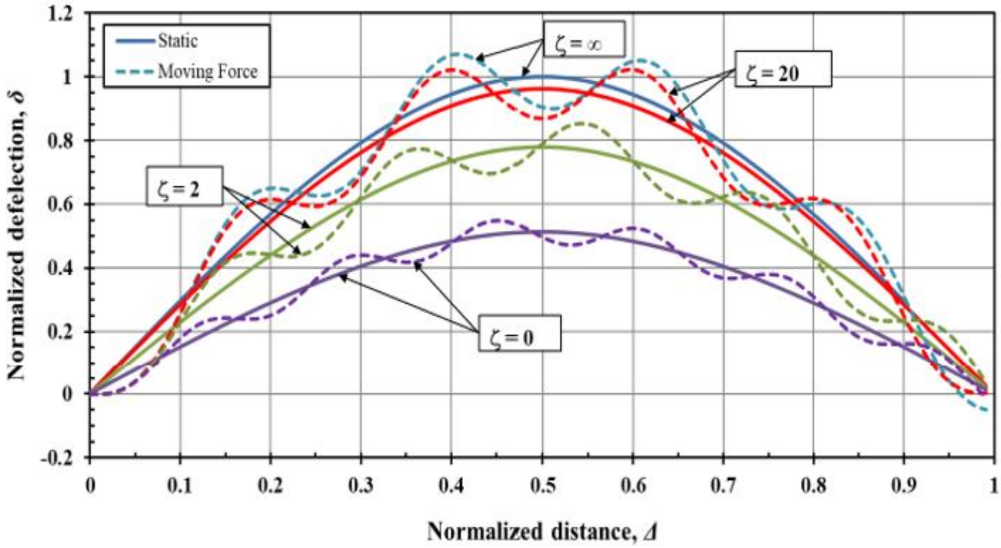

(b) Velocity = 90 km/h

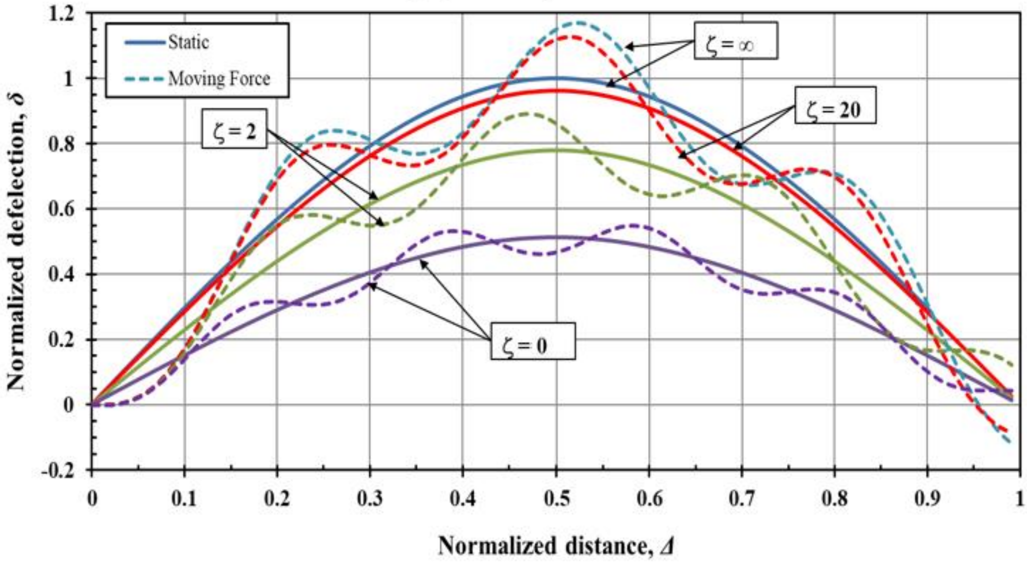

(c) Velocity = 120 km/h

Figure 8: *Normalized deflection for static load (solid line) and a moving load (dashed line) with different level of interaction* ***ζ*** *(0, 2, 20 and ∞) at different velocities, (a) 60 km/h, (b) 90 km/h and (c) 120 km/h.*

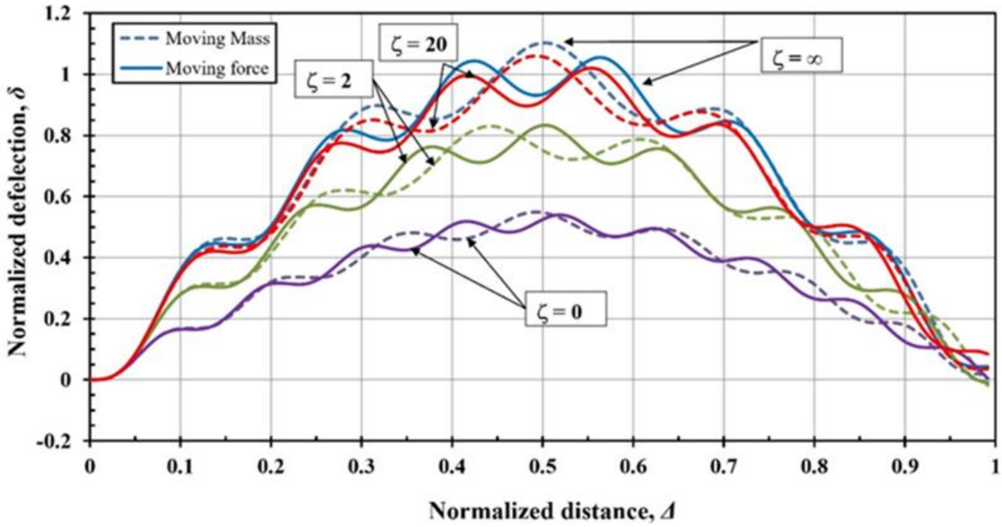

(a) Velocity = 60 km/h

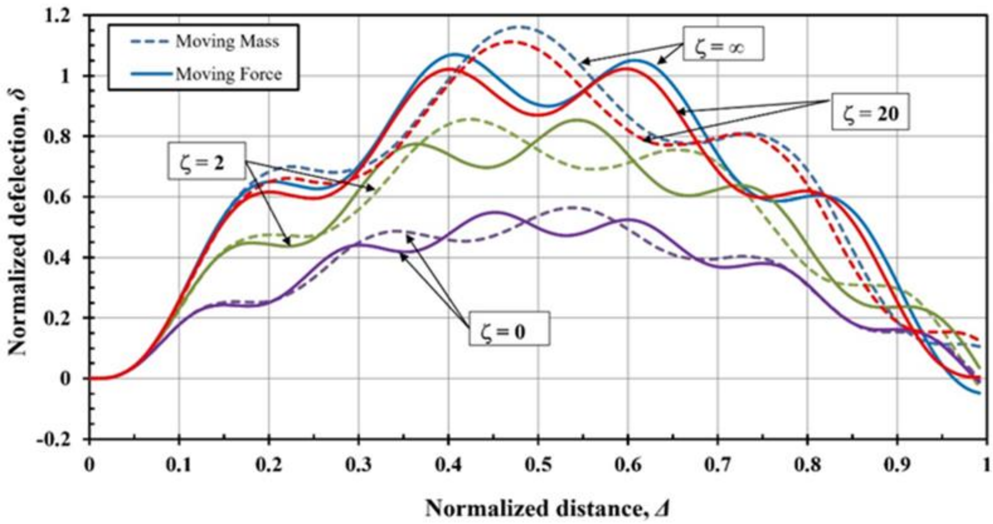

(b) Velocity = 90 km/h

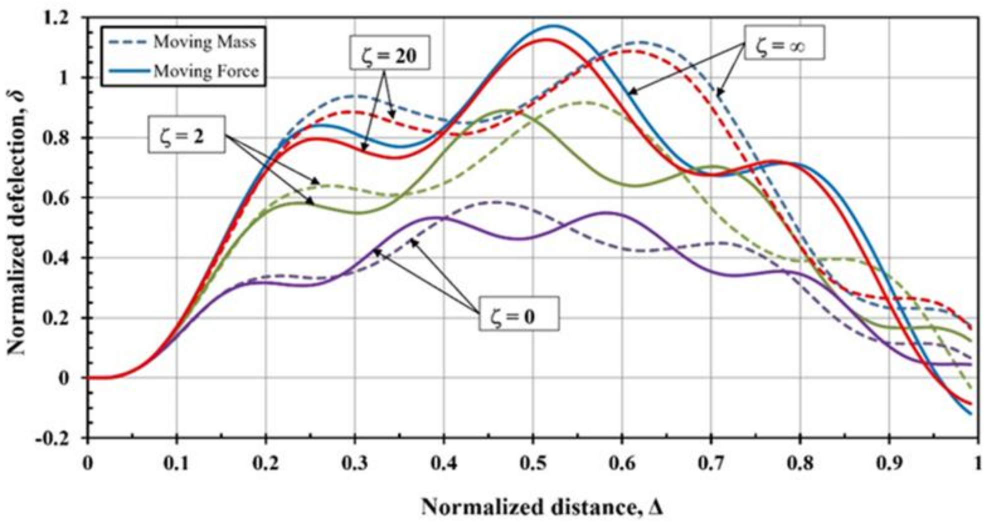

(c) Velocity = 120 km/h

Figure 9*: Normalized deflection for moving force and moving mass with different level of interaction* $\boldsymbol{\zeta}$ *(0, 2, 20 and ∞) at different velocities, (a) 60 km/h, (b) 90 km/h and (c) 120 km/h.*

4.2. Dynamic Impact Factor

Figures 10 and 11 show the dynamic impact factor (the ratio of the maximum deflection obtained in dynamic loading to the one obtained in static loading) in terms of moving force and moving mass velocities, for various levels of interaction. The impact factor increases with the increase of the moving force velocity, as would be predicted, especially at high levels of interaction. Referring to the equations (25, 26 and 27) for some cases of interaction levels ζ, the change of the impact factor can be explained for moving mass (Figure 11) does not behave similarly compared to the moving force (Figure 10), and this change is due to the consideration of the mass effect into the moving load.

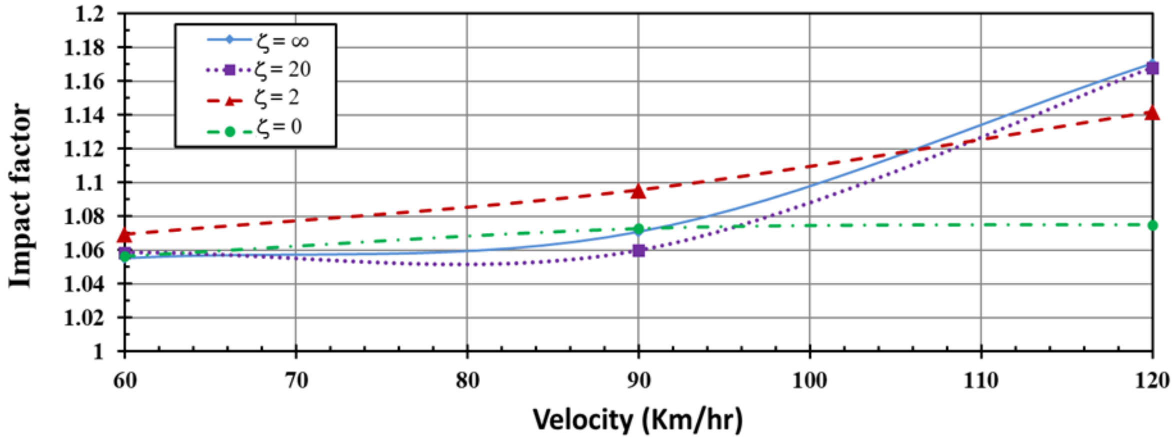

***Figure 10**: Dynamic impact factor for various moving force velocities and several levels of interaction.*

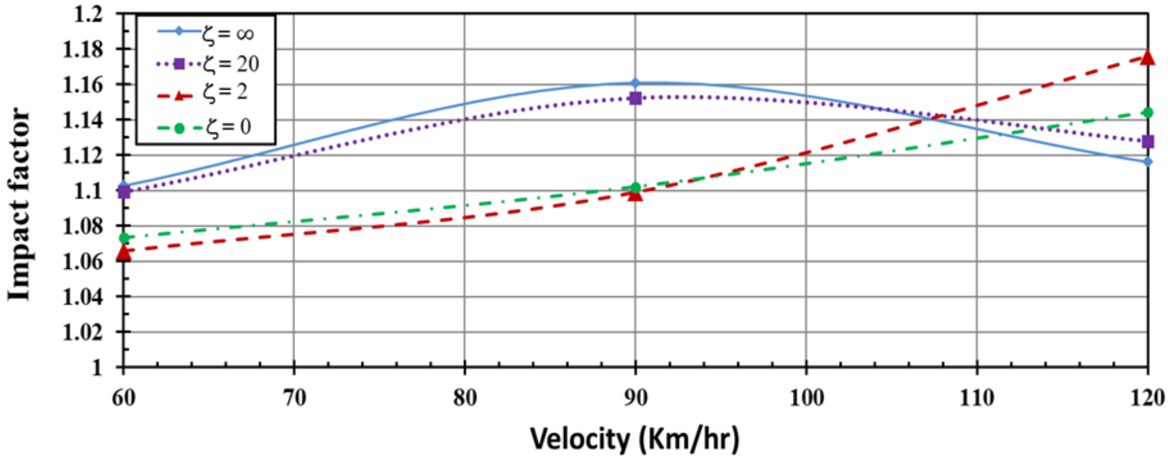

***Figure 11**: Dynamic impact factor for various moving mass velocities and several levels of interaction.*

5. CONCLUSIONS

A numerical model based on a lumped system, combining the transfer matrix method (TMM) and the analog beam method (ABM), is proposed to represent the dynamic behavior of elastic composite beam. The dynamic responses of simply supported steel-concrete composite beams with various levels of interaction between sub-beams, subjected to moving loads at different velocities, are carried out in this study. Based on the results, the following conclusions are drawn:

The proposed model is verified via comparative analyses with previous studies from literature and is applied to study the dynamic response of elastic composite beams subjected to moving load. The dynamic behavior of steel concrete composite beam is highly dependent on the level of interaction between sub-beams, the dynamic nature of the load and the load velocity. The consideration of the dynamic response of composite beams is critical, since the maximum deflections observed for the case of a moving load become up to 18% higher when compared to static loads. The consideration of the moving load as a moving mass is significant since a higher dynamic impact factor is observed at lower velocities of the mass compared to the case of moving force.

BIBLIOGRAPHIC REFERENCES

1. Biggs, J.M., Suer, H.S., et Louw, J.M. (1957). The vibration of simple span bridges. ASCE Journal of the Structural Division, 83(2), 1186–1232. https://doi.org/10.1061/JSDEAG.0000097
2. Timoshenko S., Young D. H. and Weaver W. (1974). Vibration Problems in Engineering. John Wiley, New York, fourth edition.
3. Wang, T.L., Huang, D., et Shahawy, M. (1992). Dynamic response of multi-girder bridges. ASCE Journal of Structural Engineering, 118(8), 2222–2238. https://doi.org/10.1061/(ASCE)0733-9445(1992)118:8(2222)
4. Chatterjee, P.K., Datta, T.K., et Surana, C.S. (1994). Vibration of suspension bridges under vehicular movements. ASCE Journal of Structural Engineering, 120(3), 681–703. https://doi.org/10.1061/(ASCE)0733-9445(1994)120:3(681)
5. Lin Y. H. and Trethewey M. W. (1990). Finite element analysis of elastic beams subjected to moving dynamic loads, Journal of Sound and Vibration, 136(2), 323–342. https://doi.org/10.1016/0022-460X(90)90860-3
6. Fafard, M., Bennur M., Savard. M. (1997). A general multi-axle vehicle model to study the bridge–vehicule interaction. Engineering Computations, 14(5), 491-508. https://doi.org/10.1108/02644409710170339
7. Kahya, V. (2012). Dynamic analysis of laminated composite beams under moving loads using finite element method. Nuclear Engineering and Design, 243, 41–48. https://doi.org/10.1016/j.nucengdes.2011.12.015
8. He G., Yang X. (2015). Dynamic analysis of two-layer composite beams with partial interaction using a higher order beam theory. International Journal of Mechanical Sciences, Volume 90,Pages 102-112. https://doi.org/10.1016/j.ijmecsci.2014.10.020.
9. Hongliang W., Eryu Z. (2018). Dynamic response analysis of monorail steel-concrete composite beam-train interaction system considering slip effect. Engineering Structures. 160, 257-269. https://doi.org/10.1016/j.engstruct.2018.01.037
10. Ban H, Bradford M. (2013). Flexural behaviour of composite beams with high strength steel. Engineering Structures, 56, 1130–41. https://doi.org/10.1016/j.engstruct.2013.06.040
11. Qassim, H. J., & Mohamad Ali, A. A. (2021). Dynamic response of horizontally curved composite steel I-girder bridges. Materials Today: Proceedings, 42, 1973–1979. https://doi.org/10.1016/j.matpr.2020.12.244
12. He, W. Y., Li, J. F., Cheng, H. C., Li, Z. B., & Bu, J. Q. (2022). Flexibility matrix identification using the moving vehicle induced responses for beam type bridge. Engineering Structures, 261, 114277. https://doi.org/10.1016/j.engstruct.2022.114277
13. Wang, S., Fang, Z., Ma, Y., Jiang, H., & Zhao, G. (2022). Parametric investigations on shear behavior of perforated transverse angle connectors in steel–concrete composite bridges, Structures, 38, 416–434. https://doi.org/10.1016/j.istruc.2022.01.015
14. Jiang H, Fang H, Liu J, Fang Z, Zhang J. (2021). Experimental investigation on shear performance of transverse angle shear connectors. Structures, 33, 2050–2060. https://doi.org/10.1016/j.istruc.2021.05.071
15. Ataei A., Zeynalian M., Yazdi Y. (2019). Cyclic behaviour of bolted shear connectors in steel-concrete composite beams. Engineering Structures, 198, 109455. https://doi.org/10.1016/j.engstruct.2019.109455
16. Zhang Y., Liu B., Liu H., LI Y., Zhang Y. (2017). Experimental research on the dynamic responses of the steel-concrete composite beams under the harmonic forces, Procedia Engineering, 199, 2997 - 3002. https://doi.org/10.1016/j.proeng.2017.09.392
17. Ranzi, G, M. A. Bradford, B. Uy. (2003). A general method of analysis of composite beams with partial interaction, Steel and Composite Structures, 3(3), 169-184. https://doi.org/10.12989/scs.2003.3.3.169
18. Gjelsvik A., (1991). Analog-beam method for determining shear-lag effects. Journal of Engineering Mechanics. 117(7), 1575-1594. https://doi.org/10.1061/(ASCE)0733-9399(1991)117:7(1575)
19. Betti. R, and Gjelsvik A. (1996). Elastic composite beams, Computers and Structures, 59(3), 437-451. https://doi.org/10.1016/0045-7949(95)00275-8
20. Ellakany, A., Elawadly, K., & Alhamaky, B. (2004). A combined transfer matrix and analogue beam method for free vibration analysis of composite beams. Journal of Sound and Vibration, 277(4–5), 765–781. https://doi.org/10.1016/j.jsv.2003.09.052

21. Hu, D., Wang, Y., & Ding, F. (2020). Deflection Calculation of Steel-Concrete Composite Beams Considering Effects of Shear Lag and Slip. IOP Conference Series. https://doi.org/10.1088/1757-899x/772/1/012063
22. Zhang, Y., Zhang, L. & Zhang, S. (2022). Exact series solutions of composite beams with rotationally restrained boundary conditions: static analysis. Arch Appl Mech 92, 3999–4015. https://doi.org/10.1007/s00419-022-02277-0
23. Pestel E. C., Leckie F.A. (1963). Matrix Methods in Elastomechanics, McGraw-Hill, New York, first edition.
24. Ellakany A. M. (2008). Calculation of higher natural frequencies of simply supported elastic composite beams using Riccati matrix method, Meccanica, 43, 523-532. https://doi.org/10.1007/s11012-008-9131-9
25. Ellakany A. M. and Tablia H.A. (2010). A numerical model for static and free vibration analysis of elastic composite beams with end shear restraint, Meccanica, 45(5), 523-532. https://doi.org/10.1007/s11012-009-9268-1
26. Ellakany A. M., Ali M., El-Gohary M., Elkholy M. (2019). Lumped system model for elastic steel-concrete beams with partial interaction. Multidiscipline Modeling in Materials and Structures, 16(1), 121-133. https://doi.org/10.1108/MMMS-01-2019-0007
27. Kozar I., Stimac I. (2003). Dynamic Analysis of Loads Moving Over Structures. Fourth International Congress of Croatian Society of Mechanics, Bizovac, Croatia.
28. Johansson, C., Pacoste, C., & Karoumi, R. (2013). Closed-form solution for the mode superposition analysis of the vibration in multi-span beam bridges caused by concentrated moving loads, Computers & Structures, 119, 85–94. https://doi.org/10.1016/j.compstruc.2013.01.003
29. Wang, B., Huang, Q., Liu, X. and Li, W. (2017). Experimental investigation of steel-concrete composite beams with different degrees of shear connection under monotonic and fatigue loads, Advances in Structural Engineering, 2(2), 227-240. https://doi.org/10.1177/136943321771